

Interfacial Rheology of Petroleum Asphaltenes at the Oil–Water Interface

P. Matthew Spiecker and Peter K. Kilpatrick*

Department of Chemical Engineering, North Carolina State University,
Raleigh, North Carolina 27695

Received September 2, 2003. In Final Form: February 24, 2004

A biconical bob interfacial shear rheometer was used to study the mechanical properties of asphaltenic films adsorbed at the oil–water interface. Solutions of asphaltenes isolated from four crude oils were dissolved in a model oil of heptane and toluene and allowed to adsorb and age in contact with water. Film elasticity (G') values were measured over a period of several days, and yield stresses and film masses were determined at the end of testing. The degree of film consolidation was determined from ratios of $G'/$ film mass and yield stress/ G' . Asphaltenes with higher concentrations of heavy metals (Ni, 330–360 ppm; V, 950–1000 ppm), lower aromaticity (H/C, 1.24–1.29), and higher polarity (N, 1.87–1.99) formed films of high elasticity, yield stress, and consolidation. Rapid adsorption kinetics and G' increases were seen when asphaltenes were near their solubility limit in heptane–toluene mixtures (~50% (v/v) toluene). In solvents of greater aromaticity, adsorption kinetics and film masses were reduced at comparable aging times. Poor film forming asphaltenes had yield stress/ G' values ($(1.01–1.21) \times 10^{-2}$) more than 4-fold lower than those of good film forming asphaltenes. *n*-heptane asphaltenes fractionated by filtering solutions prepared at low aromaticity (~40% toluene in mixtures of heptane and toluene) possessed higher concentrations of heavy metals and nitrogen and higher aromaticity. The less soluble fractions of good film forming asphaltenes exhibited enhanced adsorption kinetics and higher G' and yield stress values in pure toluene. Replacing the asphaltene solutions with neat heptane–toluene highlighted the ability of films to consolidate and become more elastic over several hours. Adding resins in solution to a partially consolidated film caused a rapid reduction in elasticity followed by gradual but modest consolidation. This study is among the first to directly relate asphaltene chemistry to adsorption kinetics, adsorbed film mechanical properties, and consolidation kinetics.

Introduction

Interfacial phenomena control the properties of emulsions and foams in the pharmaceutical, food products, cosmetics, and petroleum industries. Studying the rheology of emulsions and foams can provide valuable information concerning bulk viscosity, shear properties, and other end use issues. The knowledge gained by investigating interfacial properties, however, is considerably more revealing than the information available from bulk emulsions. From interfacial studies, one can determine the fundamental mechanisms and kinetics of film formation, surfactant adsorption, and film rupture that ultimately govern emulsion behavior.

Various techniques exist for the study of adsorption and rheological properties of complex surface-active molecules at air–water and oil–water interfaces.^{1–5} Benjamins et al. have nondestructively measured the viscoelastic modulus in the compression and expansion of protein films at air–water and oil–water interfaces using a dynamic drop tensiometer and a barrier plate apparatus.² They

found that increased protein adsorption time leads to an enhanced dilatational elastic modulus for both interfacial tensiometers. Inokuchi investigated the elastic and viscoelastic films formed by 6-nylon at an air–water interface with a trough device.⁶ The films were characterized according to the degree of compression: Hookian elasticity at large areas and viscoelasticity at small areas with instantaneous elasticity, delayed elasticity, and stationary flow under constant applied stress. These studies highlight the robustness of the interfacial rheometric techniques for studying the adsorption of various adsorbates at different types of interfaces.

Of extreme importance in the petroleum industry is the formation of highly viscous water-in-oil emulsions. Crude oil is found in reservoirs along with water or brine, and during oil removal, water is often coproduced. Water is also injected into the crude to remove salts or injected as steam to improve fractionation.⁷ Petroleum emulsions (typically water-in-oil^{8–11}) readily form with water in the highly turbulent nozzles and piping used for oil production. These emulsions increase pumping and transportation

* Corresponding author.

(1) Benjamins, J.; Vader, F. V. The Determination of the Surface Shear Properties of Adsorbed Protein Layers. *Colloids Surf.* **1992**, *65* (2–3), 161–174.

(2) Benjamins, J.; Cagna, A.; Lucassen-Reynders, E. H. Viscoelastic properties of triacylglycerol/water interfaces covered by proteins. *Colloids Surf., A* **1996**, *114*, 245–254.

(3) Nino, M. R. R.; et al. Surface Dilational Properties of Protein and Lipid Films at the Air–Water Interface. *Langmuir* **1998**, *14* (8), 2160–2166.

(4) Dufour, E.; Dalgalarondo, M.; Adam, L. Conformation of beta-lactoglobulin at an oil/water interface as determined from proteolysis and spectroscopic methods. *J. Colloid Interface Sci.* **1998**, *207* (2), 264–272.

(5) Ybert, C.; di Meglio, J. M. Study of Protein Adsorption by Dynamic Surface Tension Measurements: Diffusive Regime. *Langmuir* **1998**, *14* (2), 471–475.

(6) Inokuchi, K. Rheology of Surface Films IV. Viscoelastic Properties of 6-Nylon Films at Air/Water Interface. *Bull. Chem. Soc. Jpn.* **1955**, *28* (7), 453–465.

(7) Grace, R. Commercial Emulsion Breaking. In *Emulsions: Fundamentals and Applications in the Petroleum Industry*; Schramm, L. L., Ed.; American Chemical Society: Washington, DC, 1992; pp 313–339.

(8) Obah, B. The Chemical Demulsification of Crude Oil Emulsion: Problem in a Niger Delta Oil Terminal. *Erdoel Kohle, Erdgas, Petrochem.* **1988**, *41* (2), 71–74.

(9) Neumann, H. Investigations Regarding the Separation of Crude Oil Emulsions. *Petrochem* **1965**, *18*, 776–779.

(10) Eley, D. D.; et al. Electron Micrography of Emulsions of Water in Crude Petroleum. *J. Colloid Interface Sci.* **1976**, *54* (3), 462–466.

(11) Taylor, S. E. Resolving Crude Oil Emulsions. *Chem. Ind.* **1992**, *20*, 770–773.

expenses, they corrode pipes, pumps, production equipment, and distillation columns, and they poison downstream refinery catalysts.¹² It is well recognized that emulsion stability arises from the formation of an elastic interfacial film.^{12–18} Soluble aggregates from the oleic phase adsorb at the oil–water interface and present a physical barrier to flocculation and coagulation of the dispersed phase droplets. Researchers have linked interfacial film and emulsion forming behavior to petroleum asphaltenes and their interplay with resins as a solubilizing agent.^{10–12,14–16,19–31}

Asphaltenes are a solubility class of molecules found in the low-volatility portion of crude oil that forms aggregates in crude oil solvated by resins.^{32–35} Asphaltenes are defined as the portion of crude oil that is insoluble in *n*-alkanes such as *n*-heptane or *n*-pentane yet soluble in benzene or toluene.^{36,37} Asphaltenes are characterized by fused ring

aromaticity, small aliphatic side chains, and polar heteroatom-containing functional groups. Number average molecular weights by vapor pressure osmometry range from ~700 to ~3000 Da.^{33,38–44} Many studies have indicated the presence of carboxylic acid, carbonyl, phenol, pyrrole, and pyridine functional groups in asphaltenes.^{45–49} These heteroatom-containing groups are capable of donating or accepting protons inter- and intramolecularly. The most plausible mechanisms of asphaltene aggregation involve π – π overlap between aromatic sheets, hydrogen bonding between functional groups, and other charge transfer interactions. The degree to which aggregate sizes vary is controlled by the polydispersity and chemistry of the individual asphaltene monomers.

Miller and co-workers provide a comprehensive review of both tested and novel methods for probing interfacial dilatational and shear properties of adsorption layers at liquid interfaces.⁵⁰ They describe devices that measure surface velocity profiles (indirect methods) or determine torsional stress values (direct methods). Indirect techniques such as canal surface viscometers, deep channel surface viscometers, and rotating wall knife edge surface viscometers require measurements of fluid flow using easily visible inert particles from which surface viscosities can be determined. In direct methods, however, a pendulum is placed at the interface containing surfactant and it measures the torque generated after the application of an oscillatory stress.⁵¹ The biconical disk or bob interfacial viscometer is a modification of the flat disk viscometer. In each case, a stress is applied to the interface by oscillating the cylindrical cup containing the fluids. This stress in turn confers motion to the bob that is generally monitored through deflection of incident light on the torsion wire. Wibberly employed biconical bob viscometry to the study of aqueous potassium arabate–

(12) Shetty, C. S.; Nikolov, A. D.; Wasan, D. T. Demulsification of Water in Oil Emulsions Using Water Soluble Demulsifiers. *J. Dispersion Sci. Technol.* **1992**, *13* (2), 121–133.

(13) Blair, C. M. Interfacial Films Affecting the Stability of Petroleum Emulsions. *Chem. Ind.* **1960**, 538–544.

(14) Little, R. C. Breaking Emulsions of Water in Navy Fuel Oils. *Fuel* **1974**, *53* (10), 246–252.

(15) Mackay, G. D. M.; et al. The Formation of Water-in-Oil Emulsions Subsequent to an Oil Spill. *J. Inst. Pet.* **1973**, *59* (568), 164–172.

(16) Strassner, J. E. Effect of pH on Interfacial Films and Stability of Crude Oil-Water Emulsions. *J. Pet. Technol.* **1968**, *20*, 303–312.

(17) Dodd, C. G. The Rheological Properties of Films at Crude Petroleum–Water Interfaces. *J. Phys. Chem.* **1960**, *64* (5), 544–550.

(18) Graham, D. E.; Stockwell, A.; Thompson, D. G. Chemical Demulsification of Produced Crude Oil Emulsions. In *Chemicals in the Oil Industry*; Ogden, P. H., Ed.; Royal Society of Chemistry: Sunbury-on-Thames, Middlesex, U.K., 1983; pp 73–91.

(19) Johansen, E. J.; et al. Water-in-Crude Oil Emulsions from the Norwegian Continental Shelf Part I. Formation, Characterization and Stability Correlations. *Colloids Surf.* **1989**, *34*, 353–370.

(20) Cratin, P. D. A Quantitative Characterization of pH-Dependent Systems. *Ind. Eng. Chem.* **1969**, *61* (2), 35–45.

(21) Oren, J. J.; MacKay, G. D. M. Electrolyte and pH Effect on Emulsion Stability of Water-in-Petroleum Oils. *Fuel* **1977**, *56* (10), 382–384.

(22) Mansurov, I. R.; Il'yasova, E. Z.; Vygovskoi, V. P. Shear Strength of Interfacial Films of Asphaltenes. *Chem. Technol. Fuels Oils* **1987**, *23* (1–2), 96–98.

(23) Siffert, B.; Bourgeois, C.; Papirer, E. Structure and Water-Oil Emulsifying Properties of Asphaltenes. *Fuel* **1984**, *63* (6), 834–837.

(24) Menon, V. B.; Wasan, D. T. Coalescence of Water-in-Shale Oil Emulsions. *Sep. Sci. Technol.* **1984**, *19* (8–9), 555–574.

(25) Mukherjee, S.; Kushnick, A. P. Effect of Demulsifiers on Interfacial Properties Governing Crude Oil Demulsification. Presented at Symposium On Advances in Oil Field Chemistry; American Chemical Society, The Division of Petroleum Chemistry, Toronto, Canada, 1988.

(26) Isaacs, E. E.; et al. Electroacoustic Method for Monitoring the Coalescence of Water-in-Oil Emulsions. *Colloids Surf.* **1990**, *46*, 177–192.

(27) Waarden, M. v. d. Stability of Emulsions of Water in Mineral Oils Containing Asphaltenes. *Kolloid Z. Z. Polym.* **1958**, *156* (2), 116–122.

(28) Hassander, H.; Johansson, B.; Tornell, B. The Mechanism of Emulsion Stabilization by Small Silica (Ludox) Particles. *Colloids Surf.* **1989**, *40*, 93–105.

(29) Papirer, E.; et al. Chemical Nature of Water/oil Emulsifying Properties of Asphaltenes. *Fuel* **1982**, *61*, 732–734.

(30) Aveyard, R.; et al. The Resolution of Water-in-Crude Oil Emulsions by the Addition of Low Molar Mass Demulsifiers. *J. Colloid Interface Sci.* **1990**, *139* (1), 128–138.

(31) Lawrence, A. S. C.; Killner, W. Emulsions of Seawater in Admiralty Fuel Oil with Special Reference to their Demulsification. *J. Inst. Pet.* **1948**, *34*, 281.

(32) McLean, J. D.; Kilpatrick, P. K. Effects of Asphaltene Solvency on Stability of Water-in-Crude Oil Emulsions. *J. Colloid Interface Sci.* **1997**, *189*, 242–253.

(33) Al-Jarrah, M. M. H.; Al-Dujaili, A. H. Characterization of Some Iraqi Asphalts II. New Findings on the Physical Nature of Asphaltenes. *Fuel Sci. Technol. Int.* **1989**, *7* (1), 69–88.

(34) Reynolds, J. G.; Biggs, W. R. Effects of Asphaltene Precipitation and a Modified D 2007 Separation on the Molecular Size of Vanadium- and Nickel-Containing Compounds in Heavy Residua. *Fuel Sci. Technol. Int.* **1986**, *4* (6), 749–777.

(35) Nghiem, L. X.; et al. Efficient Modeling of Asphaltene Precipitation. Presented at the 68th Annual Technical Conference and Exhibition of the Society of Petroleum Engineers, Houston, TX, 1993.

(36) Mitchell, D. L.; Speight, J. G. The Solubility of Asphaltenes in Hydrocarbon Solvents. *Fuel* **1973**, *52* (4), 149–152.

(37) Yen, T. F.; Erdman, J. G.; Pollack, S. S. Investigation of Structure of Petroleum Asphaltenes by X-ray Diffraction. *Anal. Chem.* **1961**, *33* (11), 1587–1594.

(38) Acevedo, S.; et al. Asphaltenes and Resins From the Orinoco Basin. *Fuel* **1985**, *64*, 1741–1747.

(39) Boduszynski, M. M. Composition of Heavy Petroleum. 2. Molecular Characterization. *Energy Fuels* **1988**, *2* (5), 597–613.

(40) Wiehe, I. A.; Liang, K. S. Asphaltenes, Resins, and other petroleum macromolecules. *Fluid Phase Equilib.* **1996**, *117* (1–2), 201–210.

(41) McKay, J. F.; et al. Petroleum Asphaltenes: Chemistry and Composition. In *Analytical Chemistry of Liquid Fuel Sources*; Uden, P. C., Siggia, S., Eds.; Advances in Chemistry Series 170; American Chemical Society: Washington DC, 1978; pp 128–142.

(42) Andersen, S. I.; Keul, A.; Stenby, E. Variation in composition of subfractions of petroleum asphaltenes. *Pet. Sci. Technol.* **1997**, *15* (7–8), 611–645.

(43) Yarranton, H. W.; Masliyah, J. H. Molar Mass Distribution and Solubility Modeling of Asphaltenes. *AIChE J.* **1996**, *42* (12), 3533–3543.

(44) Yarranton, H. W.; Alboudwarej, H.; Jakher, R. Investigation of asphaltene association with vapor pressure osmometry and interfacial tension measurements. *Ind. Eng. Chem. Res.* **2000**, *39* (8), 2916–2924.

(45) Barbour, R. V.; Petersen, J. C. Molecular Interactions of Asphalt: An Infrared Study of the Hydrogen-Bonding Basicity of Asphalt. *Anal. Chem.* **1974**, *46* (2), 273–277.

(46) Boduszynski, M. M.; McKay, J. F.; Latham, D. R. Asphaltenes, Where Are You? *Proc. Assoc. Asphalt Paving Technol.* **1980**, *49*, 123–143.

(47) Ignasiak, T.; Strausz, O. P.; Montgomery, D. S. Oxygen Distribution and Hydrogen Bonding in Athabasca Asphaltene. *Fuel* **1977**, *56*, 359–365.

(48) Moschopedis, S. E.; Speight, J. G. Investigation of Hydrogen Bonding by Oxygen Functions in Athabasca Bitumen. *Fuel* **1976**, *55*, 187–192.

(49) Petersen, J. C. An Infra-red Study of Hydrogen Bonding in Asphalt. *Fuel* **1967**, *46*, 295–305.

(50) Miller, R.; et al. Dilational and Shear Rheology of Adsorption Layers at Liquid Interfaces. *Colloids Surf., A* **1996**, *111*, 75–118.

(51) Langmuir, I. *Science* **1936**, *84*, 303.

air and liquid paraffin interfaces.⁵² The apparatus consisted of a biconical brass bob with a 5.621 cm diameter and with an included angle of 20°. The bob was suspended by a copper beryllium wire with a known torsion constant and moment of inertia. An optical lever of 2.7 m measured the torsional displacement of the bob when subjected to an oscillation. They found the films were pseudoplastic in nature and became more rigid with time. Recently, liquid–liquid interfaces containing various polymers were studied with the biconical bob technique and a deep channel rheometer.⁵³ Comparable measurements of interfacial viscoelasticity were achieved using both rheometers, demonstrating instrument independence. Enhanced sensitivity when working with very elastic interfaces further supported the use of biconical bob rheometry.

The rheological properties of asphaltenic films, like their protein and polymer counterparts, can be probed by a variety of techniques.^{16,22,54–59} Biconical bob rheometry has been applied to both crude oil–water and model oil–water interfaces.^{57,60–62} Cairns et al. employed a biconical bob rheometer to study the interfacial viscosities of crude oil–water films.⁶⁰ They found that viscosity increased with the aging time of the interface severalfold from 2 to 6 h and suggested the presence of a viscous “interphase”. Gradual increases over several days were attributed to changes in solvent character, while multilayer formation caused the larger increases at short times. Acevedo et al. examined the shear viscoelasticity and creep compliance of Cerro Negro crude oil and asphaltenes diluted in xylene using the biconical bob rheometer of Cairns.⁵⁷ High interfacial elasticities, rather than viscosities, were purported to correlate with strong emulsions. It was again suggested that mechanically strong films result from the adsorption of aggregated asphaltenes. Mohammed and co-workers found that aging times approaching 8 h yield films with viscosities 400 times greater than those of films aged for 6 h. Beyond 8 h, the films were too rigid to deform when subjected to any applied stress.⁶² Jeribi et al.⁶³ investigated the adsorption kinetics (namely the char-

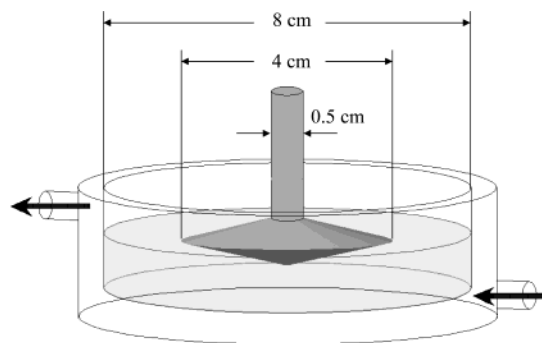


Figure 1. Schematic of the biconical bob and the associated cup for rheological measurements.

acteristic time for interfacial reorganization of adsorbed species) of asphaltene solutions via an interfacial tensiometer. At asphaltene concentrations <5 wt % in toluene and mixtures of heptane and toluene, this characteristic time ranged between 8 and 25 min. Interface deformity and rigid skins were observed at high concentrations (>10 wt % in toluene) after a day or so.

In this study, we have utilized a commercially available dynamic stress rheometer with a stainless steel biconical bob to probe interfacial film viscoelasticity. As we will show, the film properties compare well with measures of emulsion stability on systems with comparable composition. Thus, this technique provides useful insight into the mechanisms of emulsion stability in asphaltenic films and into the effects of asphaltene solvency and chemistry on interfacial adsorption.

Experimental

Asphaltene Precipitation and Fractionation. All organic solvents were HPLC grade and were obtained from Fisher Scientific. Petroleum asphaltenes were precipitated from four crude oils with a 40:1 excess of *n*-heptane. The crude oils B6 (offshore California), Hondo (HO, offshore California), Arab Heavy (AH, Safaniya), and Canadon Seco (CS, Argentina) were chosen for their high asphaltene content. Heptane precipitated asphaltenes were divided into more and less soluble fractions by dissolving them in toluene and inducing partial precipitation with heptane. Asphaltene solubilities (pre- and postfractionation) were determined in mixtures of heptane and toluene by filtration. Fractionation and solubility measurements were performed at a solute concentration of 0.75% w/v. Details of these procedures can be found elsewhere.⁶⁴

Interfacial Film Formation: Asphaltenes. The oil–water interfacial film studies were performed using a TA Instruments AR-1000 stress rheometer (TA Instruments, 109 Lukens Drive, New Castle, DE 19720). Two sample cups were developed for holding the oil and water phases. A glass sample cell with exterior water circulation was fashioned from precision bore Pyrex tubing with an interior diameter of 8 cm and a depth of 2 cm (Figure 1). The temperature was maintained at 25 °C by circulating water from a Fisher Scientific Isotemp 1016P programmable water bath. The second cup was machined from an ingot of Teflon of the same interior dimensions. This cup version did not have water circulation and was temperature controlled by the rheometer’s water-cooled Peltier plate. Both sample cells were designed to sit on top of the Peltier plate assembly and were held in place during the course of the experiment. A biconical bob similar in design to those of Shotton et al.⁶⁵ and Cairns et al.⁶⁰ for measuring interfacial rheological properties was machined from 316 stainless steel. The lower part of the bob immersed in the two phases was designed to be as thin as practically possible to reduce inertial

(52) Wibberley, K. Some Physical Properties of Interfacial Films of Potassium Arbatate. *J. Pharm. Pharmacol.* **1962**, *14*, 87T.

(53) Nagarajan, R.; Chung, S. I.; Wasan, D. T. Biconical bob oscillatory interfacial rheometer. *J. Colloid Interface Sci.* **1998**, *204* (1), 53–60.

(54) Pasquarelli, C. H.; Wasan, D. T. The Effect of Film-Forming Materials On the Dynamic Interfacial Properties In Crude Oil-Aqueous Systems. In *Surface Phenomena in Enhanced Oil Recovery*; Shah, D. O., Ed.; Plenum Press: New York, 1981; pp 237–248.

(55) Eley, D. D.; Hey, M. J.; Lee, M. A. Rheological Studies of Asphaltene Films Adsorbed at the Oil/Water Interface. *Colloids Surf.* **1987**, *24*, 173–182.

(56) Wasan, D. T. Destabilization of Water-in-Oil Emulsions. In *Emulsions—A Fundamental and Practical Approach*; Sjöblom, J., Ed.; Kluwer Academic Publishers: Dordrecht, The Netherlands, 1992; pp 283–295.

(57) Acevedo, S.; et al. Interfacial Rheological Studies of Extra-Heavy Crude Oils and Asphaltenes: Role of the Dispersion Effect of Resins in the Adsorption of Asphaltenes at the Interface of Water-in-Crude Oil Emulsions. *Colloids Surf., A* **1993**, *71*, 65–71.

(58) Mohammed, R. A.; et al. Dewatering of Crude Oil Emulsions 2. Interfacial Properties of the Asphaltic Constituents of Crude Oil. *Colloids Surf., A* **1993**, *80*, 237–242.

(59) Khristov, K.; et al. Thin liquid film technique—application to water-oil-water bitumen emulsion films. *Colloids Surf., A* **2000**, *174* (1–2), 183–196.

(60) Cairns, R. J. R.; Grist, D. M.; Neustadter, E. L. *The Effect of Crude Oil–Water Interfacial Properties on Water-Crude Oil Emulsion Stability*; Academic Press: London, 1974.

(61) Neustadter, E. L.; Whittingham, K. P.; Graham, D. E. Interfacial Rheological Properties of Crude Oil/Water Systems. In *Surface Phenomena in Enhanced Oil Recovery*; Shah, D. O., Ed.; Plenum Press: New York, 1981; pp 307–326.

(62) Mohammed, R. A.; et al. Dewatering of Crude Oil Emulsions 1. Rheological Behavior of the Crude Oil–Water Interface. *Colloids Surf., A* **1993**, *80*, 223–235.

(63) Jeribi, M.; Almir-Assad, B.; Langevin, D.; Henaut, I.; Argillier, J. F. Adsorption Kinetics of Asphaltenes at Liquid Interfaces. *J. Colloid Interface Sci.* **2002**, *256*, 268–272.

(64) Spiecker, P. M.; Gawrys, K. L.; Kilpatrick, P. K. Aggregation and solubility behavior of asphaltenes and their subfractions. *J. Colloid Interface Sci.* **2003**, *267*, 178–193.

(65) Shotton, E.; et al. A Versatile Surface Rheometer. *Rheol. Acta* **1971**, *10*, 142–152.

effects. The upper part had recessed threads to mate properly with the instrument's stress head (Figure 1). The bob was tapered from the narrow center shaft (0.5 cm diameter) out to a knife edge at the perimeter (4 cm diameter). The edge was serrated around the circumference (30°, 3 mm deep) to maintain adhesion to the film at higher applied stresses.

Before each experiment, the bob was cleaned with methylene chloride followed by water and detergent and then rinsed with deionized water. The interior of each cup was cleaned with a 7:3 (v/v) mixture of concentrated sulfuric acid and 30% hydrogen peroxide (technical grade, Fisher), the so-called "piranha" solution. (The piranha solution is extremely corrosive and highly exothermic. Prepare only as much as necessary.) This step ensured that the cup walls were free of the most stubbornly adhering organics.

Films were formed by adding a solution of asphaltenes dissolved in heptane and toluene to deionized water (HCl and NaOH adjusted to pH 6). The water phase (40 mL) was added to the sample cell first. This volume of water was chosen to provide a sufficient distance between the bob and the bottom of the glass cup (>1 cm). The bob was then lowered onto the surface of the water. Upon initial contact, the water was drawn upward toward the edge of the bob due to the high surface energy of stainless steel. As the bob was lowered, the meniscus formed between the bob edge and the water gradually diminished. The final vertical position of the bob was set when this meniscus was eliminated. Precise control of the vertical movement of the bob ensured an accurate and reproducible means for locating the position of the interface regardless of the aqueous phase volume. At this point, angular rotation of the bob was stopped mechanically. The oil phase (35 mL) was pipetted slowly onto the bob and flowed outward to minimize interfacial disturbance.

To reduce solvent evaporation, a Teflon solvent cap split into two halves was placed over the cup. A thin layer of silicon grease was applied to the edge of the glass to help seal the system. Additionally, two solvent troughs were affixed to the underside of the cap into which heptane and toluene were transferred throughout the experiment. A small gap, however, was maintained around the bob shaft to allow frictionless oscillation during testing.

Appropriate correction factors were used to control and monitor the response of the film to an applied stress. We used the approximation of Shotton et al. in which the interphase region is treated as a slice through a concentric cylinder system.⁶⁵ The instrument stress and rate factors were determined from the bob and cup dimensions and the expressions for a generic concentric cylinder geometry. These expressions appear as follows:

$$F_{\text{stress}} = \frac{R_i^2 + R_o^2}{4\pi R_i^2 R_o^2} \quad (1.1)$$

$$F_{\text{rate}} = \frac{R_i^2 + R_o^2}{R_o^2 - R_i^2} \quad (1.2)$$

where R_i and R_o are the bob radius (2 cm) and cup radius (4 cm), respectively.

In the presence of a mechanically rigid film and under low amplitude oscillatory motion, the contribution of the two nearly Newtonian fluids on the top and bottom of the bob was neglected. Thus, the resistance to applied oscillation resulted from the asphaltenic film and was gauged by the magnitudes of the elastic and viscous moduli. These moduli represented as G' (the storage modulus) and G'' (the loss modulus) are either in-phase or out-of-phase with the strain, respectively. The moduli and the sinusoidally varying stress are related by the following expression:

$$\sigma(t) = \gamma_0 [G'(\omega) \sin(\omega t) + G''(\omega) \cos(\omega t)] \quad (1.3)$$

where σ is the shear stress, γ_0 is the applied strain amplitude, and ω is the frequency of oscillation.⁶⁶ Low loss tangents ($\tan \delta = G''/G' \ll 1$) imply solidlike behavior, while high loss tangents imply liquidlike behavior. Since Newtonian liquids such as water and heptane–toluene mixtures have no inherent elasticity, their

loss tangents are accordingly high. The rigid asphaltene films, however, have much lower loss tangents.

Frequency sweeps were performed on the interface to probe the kinetics of film formation. The film was allowed to develop for at least 1 to 2 h before the initial testing. Even though there was evidence of asphaltene adsorption within minutes of the oil phase addition, there was not sufficient coverage or consolidation to impart a measurable signal when probed by the rheometer. Sheu found that dynamic toluene–water interfacial tension values measured at lower bulk asphaltene concentrations (<0.1 wt %) via a Wilhelmy plate approached equilibrium within 100 min.⁶⁷ Beyond 2 h, the interfacial tensions reached a plateau due to film formation and provided no additional information. The bulk concentration of our systems is 7.5-fold greater and less aromatic which will enhance adsorption and decrease the time to reach an equilibrium dynamic interfacial tension. At this point, the emergence of measurable film elasticity allows us to follow adsorption and film consolidation. The highly elastic film precludes the measurement of interfacial tension, since the asphaltenes will have adsorbed to the plate or the du Nouy ring apparatus.

Some slow adsorbing systems, however, required substantially more aging time before testing. Film adsorption and consolidation were monitored in some cases for as long as several days. Exploratory film experiments provided the optimum stress and frequency ranges that would yield a smooth and timely response to the applied stress. These sweeps were performed at an applied stress of 0.01 Pa (within the linear viscoelastic regime) from 0.1 to 3 rad/s. Very low applied stresses (<0.001 Pa) often produced weak signals and scattered data. The TA AR1000 transducer is not rated below 0.0008 Pa. Applied stresses that were too high often exceeded the yield stresses of the film and caused rupturing. Operating at low frequencies (<0.1 rad/s) required testing times that may have approached or exceeded the aging times. At high frequencies (>3 rad/s), high bob inertia caused erroneous data. After the final frequency sweep, a stress sweep at 1 rad/s was used to determine the film yield stress. As can be seen in the results section, the variability in values of G' , the elastic modulus, was of the order of 0.05–0.1 Pa and this is a good measure of the precision of the data.

The stress sweep was performed until the film ruptured (at either the bob edge or at the cup wall). Upon completion, the Teflon solvent cap was removed, the oil was extracted via pipet, and the bob was raised and detached from the rheometer. The remaining oil and water were both extracted to expose the film (if present). Alternating methylene chloride and acetone rinsing helped to dissolve the film from the glass. Finally, the redissolved/dispersed film material was transferred to a small vial for drying and weighing.

Results and Discussion

Rheological Behavior of a Rigid Interfacial Film.

A solution of B6 asphaltenes in 35 mL of Heptol (55% (v/v) toluene) was transferred onto the water surface, and the interface aged for 24 h. Frequency and stress sweeps were performed to obtain representative data of the adsorbed asphaltenic film. When using the transparent glass sample cup, the oil–water interface showed the signs of asphaltene adsorption after just a few minutes of aging. The interface, initially black due to the opacity of the asphaltene solution, rapidly became light brown as asphaltenes adsorbed. Adsorption quickly covered the entire interface from the biconical bob edge to the glass wall. The adsorbed asphaltenes clearly adsorbed within the gaps of the bob serrations designed to maximize adhesion to the bob edge. Initial measurements indicated that the degree of adsorption and consolidation was insufficient for rheological testing until after at least 1–2 h of aging due to the limited

(66) Larson, R. G. The structure and rheology of complex fluids. *Topics in Chemical Engineering*; Gubbins, K. E., Ed.; Oxford University Press: New York, 1999.

(67) Sheu, E. Y.; Detaar, M. M.; Storm, D. A. Interfacial Properties of Asphaltenes. *Fuel* **1992**, 71 (11), 1277–1281.

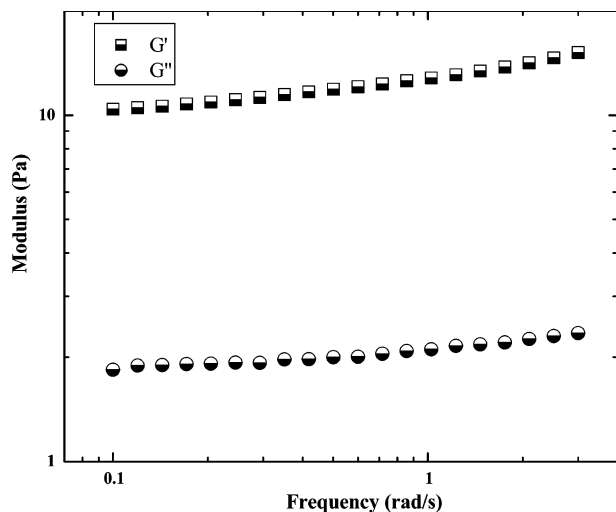


Figure 2. Measurement of G' and G'' as a function of the oscillatory shear frequency of the adsorbed film of the B6 whole asphaltenes: 0.75% w/v, 55% toluene, 0.01 Pa, 24 h.

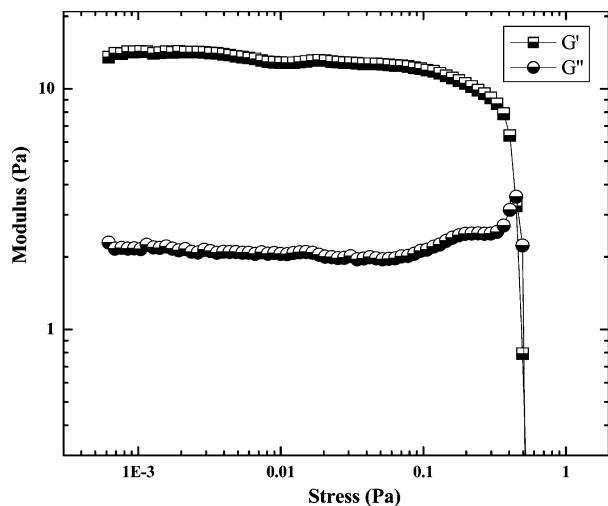


Figure 3. Measurement of G' and G'' as a function of the oscillatory shear stress of the adsorbed film of the B6 whole asphaltenes: 0.75% w/v, 55% toluene, 1 rad/s, 24 h.

sensitivity of the instrument; that is, the applied stress necessary to generate the minimum torque ($0.1 \mu\text{N m}$) was greater than the film yield stress.

Upon aging for 24 h, an oscillatory frequency sweep (Figure 2) was performed at an applied stress of 0.01 Pa from 0.1 to 3 rad/s and revealed elastic solidlike behavior in which G' increased slightly with increasing frequency and was about 1 order of magnitude greater than G'' . Frequency sweeps at very short aging times (<1 h) occasionally showed $G'-G''$ crossover in which $\tan \delta = 1$, indicating a weakly cross-linked film. The elastic nature of the more developed and aged asphaltenic films likely results from strong intermolecular interactions which cross-link the film. The 24 h frequency sweep was followed by a stress sweep (Figure 3) at 1.0 rad/s from the minimum applied stress to the yield stress. The linear viscoelastic regime extended over two decades of applied stress. As the applied stress approached the rupture point, the film began to break down, as witnessed by the sharp decrease in the elastic modulus. At the same time, the viscous modulus rose to a maximum during film rupture, likely due to pieces of film contributing to viscous stresses in the interfacial zone. When the applied stress exceeded the rupture stress, the bob ultimately spun free from the

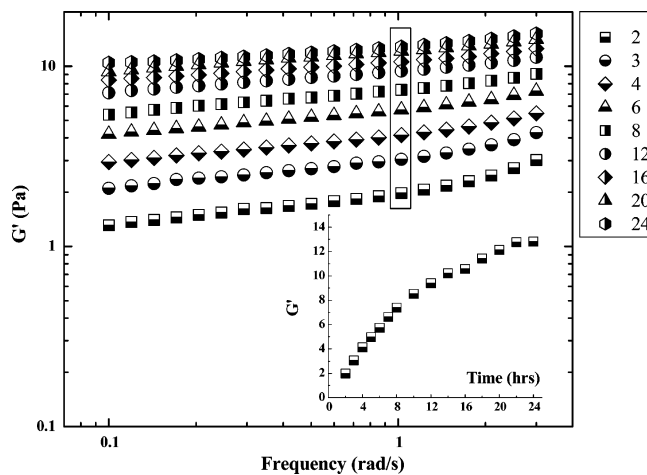


Figure 4. Measurement of G' and G'' as a function of the oscillatory shear frequency of the adsorbed films of the B6 whole asphaltenes as a function of time (adsorption time in hours): 0.75% w/v, 55% toluene, 0.01 Pa.

resisting film and G' and G'' reduced to values associated with a nonviscoelastic, asphaltene-free oil–water interface. The film typically separated from the edge of the bob and sometimes from the glass cylinder wall in all experiments. The yield stress measured for this process could be considered a lower bound on the actual yield stress due to defects in the film between asphaltenes and glass or stainless steel. Upon film rupture, the experiment was discontinued and the sample cell was cleaned. The oil phase was pipetted from the cell, exposing the light-brown film. The film had considerable resistance to probing with a pipet tip and a thickness on the order of $1 \mu\text{m}$ or more. This is inferred from measurements of the film mass reported below, and these masses assist in discerning differences in adsorption, film consolidation, and film strength.

The effect of interface aging on film elasticity is shown in Figure 4; aging increases asphaltene adsorption and consolidation that contribute to film strength. We focus on G' , as the magnitude of the elastic modulus is a reliable measure of film growth. A plot of G' versus time at an oscillatory frequency of 1 rad/s (half-filled squares) is shown in Figure 4 (inset). Between 2 and 8 h, the rate of increase in the elastic modulus was nearly constant. G' continued to increase to 24 h, whereupon the rate of growth slowly decreased. This growth process can be explained by a combination of asphaltene adsorption and consolidation. The available supply of asphaltenes in solution provides a driving force for adsorption from the bulk. The interface behaves like a sink capable of adsorbing asphaltenes in solution. It appears that, by extrapolating to zero time, G' passes through the origin (see the inset of Figure 4). As we will show below, the change in G' with time is attributable to two phenomena—adsorption of asphaltenes and molecular rearrangement or consolidation of the asphaltenes once they are at the interface. Figure 4 clearly demonstrates that this process takes 20–30 h to achieve a steady state. This is in contrast to interfacial tension measurements, such as those reported by Jeribi et al.,⁶³ in which it appears that the tension determined by drop shape analysis reaches a steady value at Heptol–water interfaces in time scales ranging from 15 to 60 min. Thus, one might infer that the rheology experiments here are probing a mechanical property which is inaccessible to interfacial tension measurements. Thus, the two methods are seen to be complementary.

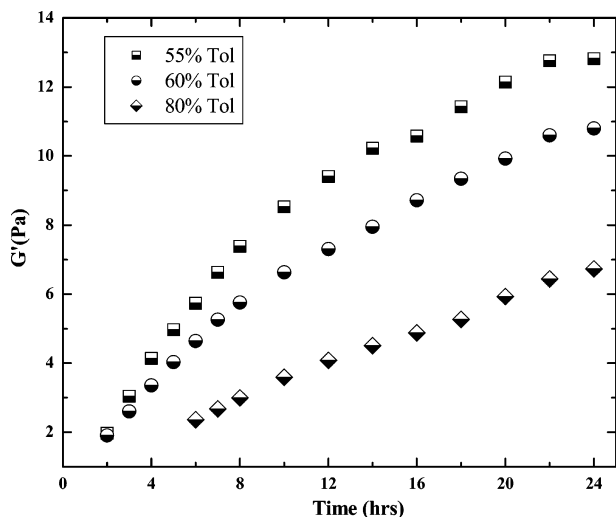


Figure 5. Kinetics of film adsorption and consolidation as probed by G' of the adsorbed films of the B6 whole asphaltenes at varying toluene concentrations in toluene–heptane solutions: 0.75% w/v, 0.01 Pa, 1 rad/s.

Asphaltene Solubility and its Effects on Film Rheology. The limits of asphaltene solubility in Heptol were determined by filtration experiments and have been reported in a previous publication;⁶⁴ all four asphaltenes studied were completely soluble above toluene volume fractions in Heptol ranging from 0.48 to 0.52. Below this toluene concentration, the fraction of precipitate increased as the ratio of heptane to toluene increased. Small angle neutron scattering (SANS) of asphaltene aggregates in Heptol solution showed that aggregate correlation lengths reached their maximum at the solubility limit. Higher toluene volume fractions reduced the degree of aggregation by solvating the aromatic moieties of asphaltene molecules and reducing intermolecular π -bonding. At the solubility limit, enhanced aggregation produced a large driving force for adsorption at oil–water interfaces. This effect was seen in the stability of water-in-oil emulsions formed with asphaltenes near their solubility limit. Well-solvated asphaltenic aggregates create much weaker emulsions than larger, interfacially active aggregates. We see this same solvent-induced adsorption effect manifested in our measurements of interfacial rheology.

Figure 5 shows the effect of solvency on film elasticity as a function of aging time. At 55% toluene, the asphaltenes formed sizable aggregates⁶⁴ and were driven to adsorb strongly. As a result, elasticity grew at a higher rate at 55% toluene than at 60 or 80% toluene, where the aggregates were better solvated and slower to adsorb at the oil–water interface. More than 5 h of aging was required at 80% toluene to ensure that a well-formed film existed that was suitable for testing. It is clear that the films had not reached their equilibrium elasticity even after 24 h and that adsorption and consolidation were still proceeding.

In contrast to the films formed by well-solvated asphaltenes, systems containing a large fraction of precipitated asphaltenes behave quite differently. In Heptol with a toluene volume fraction of 0.4, ~33% (w/w) of the asphaltenes are insoluble and form large ($>1 \mu\text{m}$) flocs. Since these flocs are not soluble and are of greater density than the oil phase, they naturally settle onto the oil–water interface. Previous studies found that emulsions formed by the isolated insoluble material, when redissolved in toluene and mixtures of heptane and toluene, were as stable as those formed by the unfractionated

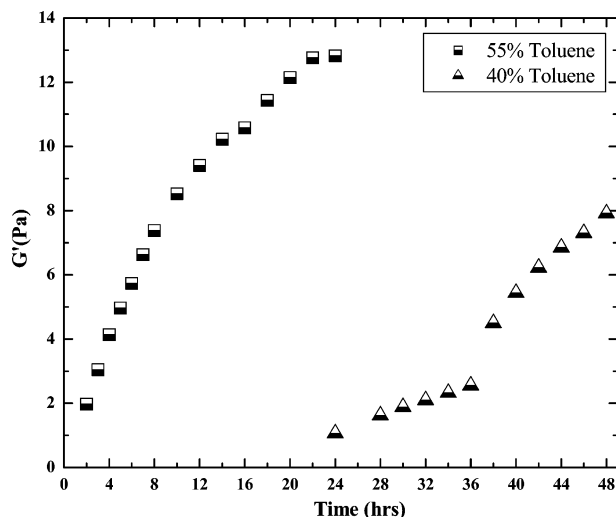


Figure 6. Kinetics of film adsorption and consolidation as probed by G' of the adsorbed films of the B6 whole asphaltenes at 40% and 55% toluene: 0.75% w/v, 0.01 Pa, 1 rad/s.

Table 1. Asphaltene Chemistry

asphaltene	fraction	solubility limit (% toluene)	ζ (Å)	H/C	N (wt %)	Ni (ppm)	V (ppm)
AH	sol	38	34.5	1.17	0.92	84	350
	whole	48	67.3	1.14	1.02	160	490
	ppt	60	130	1.13	1.08	160	540
HO	sol	45	52.3	1.30	1.95	340	930
	whole	52	72.8	1.29	1.99	360	950
B6	ppt	80	200	1.24	2.11	410	1100
	sol	42	62.7	1.30	1.81	350	1000
	whole	52	97.6	1.24	1.87	330	1000
CS	ppt	90	262	1.22	1.93	410	1200
	sol	40	138	1.12	1.32	19	42
	whole	50	246	1.11	1.32	21	48
	ppt	70	520	1.09	1.39	28	48

asphaltenes. This less soluble or “precipitated” fraction was also shown to possess a higher level of aromaticity (lower H/C), polarity (higher N), and heavy metals (Ni and V) than that of the more soluble, or “soluble” or unfractionated “whole”, asphaltenes (Table 1).⁶⁴ Thus, by inducing the flocculation of the most aromatic and polar asphaltene fraction, film formation was hindered by both a reduced amount of soluble interfacially active material and an oil–water interface covered by large flocs.

The effects of asphaltene precipitation on film formation and elasticity are shown in Figure 6. There is a considerable time lag with the 40% toluene solution, and this can likely be attributed to the presence of precipitates at the interface which impede the adsorption and consolidation of soluble asphaltenes. After 24 h, enough soluble material had adsorbed and consolidated to produce a film of measurable rheological properties. Certainly, the heavy accumulation of precipitated asphaltenes conferred some resistance to the applied stress and contributed to interfacial elasticity. The jump in G' from 36 to 38 h may be due to the formation of a partially consolidated film comprised of some soluble asphaltenes and many precipitated asphaltenes.

Two measures we adopted to facilitate comparison of film strengths formed under differing conditions were the $G'/\text{film mass}$ (or G'/mass) and yield stress/ G' (or YS/G') ratios. The ratio G'/mass differentiates films by their elasticity per unit mass, which we believe may reflect the degree of consolidation of the film. Low ratios suggest low or poor consolidation and accumulated material that is not well integrated into a coherent film. High ratios

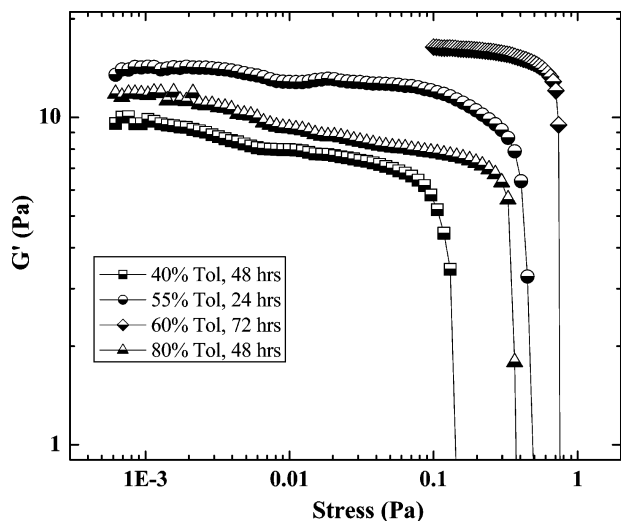


Figure 7. Stress sweeps of the B6 whole asphaltene films adsorbed at different Heptol ratios and aging times: 0.75% w/v, 1 rad/s.

Table 2. Whole Asphaltene Film Properties^a

asphaltene	% toluene	aging time (h)	G' (Pa)	yield stress (Pa)	film mass (g)	G'/mass (Pa/g)	YS/G' ($\times 10^{-3}$)
B6	40	48	7.91	0.145	0.0850	93.1	18.3
	55	24	12.82	0.497	0.0532	241	38.8
	60	72	17.22	0.770	0.0409	421	44.6
	80	48	9.18	0.365	0.0200	459	39.8
HO	55	48	5.55	0.297	0.0097	572	53.4
	60	48	3.64	0.218	0.0068	536	59.9
CS	55	48	10.51	0.106			10.1
	60	48	5.25	0.0636			12.1
AH	55	96	0.64				

^a At 0.75% w/v in Heptol, 1 rad/s frequency.

suggest greater consolidation, and films comprised of soluble and highly surface-active asphaltene aggregates are more likely to yield such high ratios. The YS/G' ratio provides an alternative measure of film consolidation and is useful when the film is not recoverable to measure film mass. The yield stress per unit elasticity probes the brittleness of the film. Stress sweeps performed on several adsorbed films of B6 whole asphaltenes immediately following the final frequency sweep are shown in Figure 7. G' is plotted as a function of applied stress at a frequency of 1 rad/s. These films were aged between 24 (55% toluene) and 72 h (60% toluene), making direct comparison difficult. However, the G'/mass and YS/G' ratios for the 40% toluene film suggest considerably lower consolidation compared to that of the films formed under more soluble conditions (see Table 2). At 40% toluene, there was a heavy accumulation of unconsolidated asphaltenes on the interface and a correspondingly high film mass. The film elasticity in this low solubility regime was the lowest of the four systems and resulted in the lowest ratio of elasticity to film mass. The second measure of film consolidation (YS/G') indicated the 40% toluene film was the weakest and the most brittle of all the B6 whole systems studied; its value of YS/G' was substantially lower than those of the other films. The precipitated material undoubtedly contributed to the lack of film consolidation, resulting in a low yield stress and YS/G' ratio. A highly consolidated film is characterized by high G'/mass and YS/G' ratios. These occur in the soluble regime with B6 whole asphaltenes. Asphaltene adsorbed from increasingly soluble solutions (higher toluene content) take much longer to achieve comparable film strengths and degrees

of consolidation as those of asphaltenes adsorbed at conditions near the solubility limit. The specific gravities of Heptol (~ 0.75), asphaltenes (~ 1.2), and water (1) lead to accumulation of asphaltene flocs on the interface because the flocs have considerable entrained solvent and are thus of intermediate density between the densities of Heptol and water. At solvency conditions near the solubility limit and in the insoluble regime, a large accumulation of asphaltenes was observed on the bob and the interface. Asphaltene adsorption and precipitation was often noticed on the bob due to the high surface energy of stainless steel and on the interface. Since it was often difficult to discriminate between asphaltene adsorbed at the interface and those precipitated or accumulated on top, G'/mass values may be underestimated. We estimate the uncertainty in the film masses to be $\pm 5\text{--}10\%$. For these reasons, the YS/G' ratio may be a better discriminator of film consolidation.

Despite the challenges associated with measuring film mass, we can infer from film mass the polarity of adsorbed asphaltene. Near the solubility limit, asphaltene aggregation is mediated by dispersive interactions between aromatic rings and polar and hydrogen bonding between functional groups. At these solvent conditions, asphaltene form aggregates of the largest dimensions⁶⁴ and are most prone to adsorb. The limited solubility drives a large percentage of asphaltene to the interface, the film mass rises, and the G'/mass ratio decreases. As the solvent becomes more aromatic, its ability to disrupt π -bonding between asphaltene aggregates is enhanced. Here, aggregation and adsorption are governed by polar and hydrogen bonding interactions. Thus, aggregates capable of adsorbing to the oil-water interface in very soluble conditions are the most polar.

In the soluble regime, above $\sim 50\%$ toluene, films have YS/G' values more than double those in the insoluble regime, presumably due to the much greater degree of consolidation. This is likely attributable to the smaller aggregate size and greater mobility of asphaltene in these more aromatic conditions. We found from the analysis of emulsions formed with asphaltene at these solvency conditions ($> 50\%$ toluene) that their stabilities were quite high. Emulsions produced at 80% toluene were slightly weaker than those produced at 55 or 60% toluene due to enhanced solubility. This can be attributed to the longer time scale required for adsorption and consolidation of sufficiently consolidated films in order to stabilize emulsion droplets.

Identifying the appropriate time scales for diffusion from the bulk to the interface enables a comparison between the kinetics of asphaltene adsorption to emulsion droplets and the kinetics at planar interfaces, as reflected by rheology. Emulsions are formed by the high energy mixing of oil and water with dissolved asphaltene and are stable after just a few seconds of mixing. In a previous study, minimum droplet diameters of a few microns were generated after tens of seconds of homogenization.⁶⁸ Sufficient adsorption times for rheological testing of planar oil-water interfaces, however, were on the order of hours. In a high internal phase ratio emulsion (50–80% dispersed phase), the distances between droplets are on the order of a few microns. Thus, the characteristic diffusion time should be

$$t_D \cong L^2/D \quad (2.1)$$

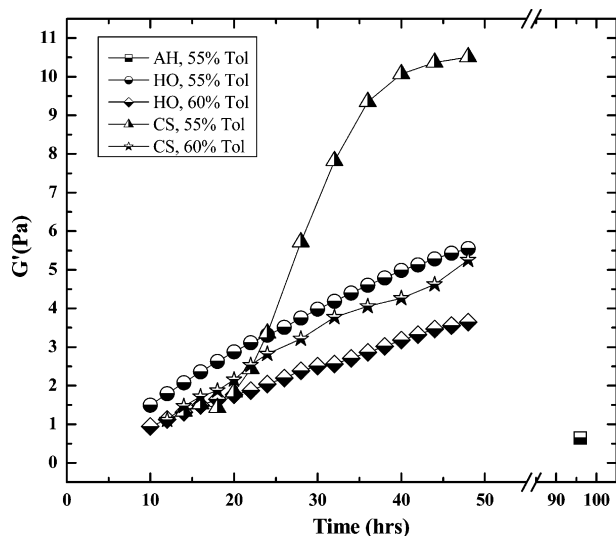


Figure 8. Kinetics of film adsorption and consolidation as probed by G' of the adsorbed films of AH, CS, and HO whole asphaltenes: 0.75% w/v, 0.01 Pa, 1 rad/s.

where L is the diffusion length and D is the asphaltene self-diffusion coefficient ($\sim 1 \times 10^{-6}$ cm²/s in toluene⁶⁹). In an emulsion, $t_D \cong 1$ s, assuming a 10 μ m diffusion length. In the case of a few tens of milliliters of asphaltene solution above water (solution depth, ~ 0.7 cm) and choosing a near-interface diffusion length of a few millimeters, the characteristic diffusion time is measured in tens of hours. Thus, the experiments performed here to understand relative variation in consolidation and strength of asphaltenic films formed over many hours of adsorption are indeed relevant to understanding the stability of emulsions.

Asphaltene Chemistry and Film Formation. Previously, we observed that B6 asphaltenes formed films of highest elasticity near the solubility limit and that the time scale required to form films of high strength increased as the goodness of the solvent increased. AH, CS, and HO asphaltene solutions (0.75% w/v) were prepared at solvency conditions near their solubility limits to study film elasticity. Films of HO and CS asphaltenes were probed from 10 to 48 h, while those of AH asphaltenes were tested once at 96 h (Figure 8). By studying the properties of films formed with asphaltenes precipitated from different crude oils, we gained a better understanding of the mechanisms of adsorption and consolidation in asphaltenic films. The chemical properties of all four asphaltenes and their more and less soluble fractions appear in Table 1. AH asphaltenes were the most soluble, formed the smallest aggregates in solution, had high aromaticity, and had low nitrogen and metal contents. CS asphaltenes formed the largest aggregates, were the most aromatic, and also had low nitrogen and metal contents. By contrast, B6 and HO were both offshore California crude oils and had chemically similar asphaltenes, including lower aromaticities and higher nitrogen and metal contents than those of AH or CS. Emulsion stability tests indicated that B6 and HO asphaltenes formed the strongest emulsions, while AH and CS asphaltenes formed emulsions considerably weaker at all conditions of solvency.

The behavior of HO asphaltenic films at 55 and 60% toluene suggested that they were similar in many respects to B6 asphaltenic films. Both HO and B6 films were light-

brown colored and quite resistant to applied stresses. However, HO required nearly 5 times longer than B6 to form sufficiently consolidated films to test rheologically and G' at 24 or 48 h was less than half that of B6 at a comparable aging time.

The film elasticities of CS asphaltenes were significantly different than comparable films of B6 and HO asphaltenes. At the conclusion of the 55 and 60% toluene experiments, the oil phases of CS solutions were removed via pipet to reveal a poorly consolidated film that could not be harvested intact. Even though CS at 55% toluene showed a substantial rise in G' between 24 and 48 h, this may be attributed to accumulated, adsorbed asphaltenic aggregates and flocs that were driven from solution after extended interfacial contact with water. This material, being confined by the glass wall and the serrated edge bob, conferred a degree of elasticity on the film but with very little consolidation. The asphaltenic aggregates were likely quite large (>250 Å), as measured by SANS in Heptol,⁶⁴ and thus were not able to form a defect-free, cohesive interfacial film.

AH asphaltenes were nearly incapable of forming a consolidated interfacial film even after 96 h of interfacial aging. SANS measurements performed on solutions at comparable bulk concentration indicated that AH asphaltenes formed the smallest aggregates of the asphaltenes examined and were very well solvated in Heptol.

In Table 2, we present film properties of AH, CS, HO, and B6 asphaltenes that shed light on the differences seen between cohesive, elastic film formers (B6 and HO) and unconsolidated film formers (AH and CS). High G'/mass and YS/G' ratios were the trademarks of well-consolidated films. HO films actually had higher G'/mass and YS/G' ratios than B6 asphaltene films but lower G' values at comparable aging times. HO asphaltenes formed smaller aggregates (73 Å) than B6 asphaltenes (98 Å) near the solubility limit, as measured by SANS, and were slightly less surface-active and weaker emulsion formers; this is consistent with the rheological data. The reduced surface activity of HO relative to B6 prevented a larger accumulation of unconsolidated asphaltenes onto the film. As a result, the film mass of HO asphaltenes was lower than that of B6 asphaltenes and the G'/mass ratio was correspondingly higher. Lower film masses and kinetics of formation also indicate that HO asphaltenes are well solvated even near the solubility limit and imply that HO is less polar and surface-active than B6.

Another interesting byproduct of high surface activity and film adsorption was the tendency of B6 films to expand in the direction of the meniscus formed between the oil-water interface and the cup wall. The contact angle between pure water and clean glass is near 0°. The oil phase pipetted on top at the beginning of the experiment naturally followed the shape of this meniscus. At times greater than 8–10 h, the film-glass interface appeared to slowly wrinkle, deform, and extend upward into the oil phase. At 48 h, this process changed the appearance of the film edge noticeably (see Figure 9). Decreased adhesion of the film to the glass surface at this stage of film aging may have reduced the yield stress and led to lower YS/G' values than those of HO films. HO films were slower to form and did not appear to exhibit the same degree of edge effects.

In contrast to the cases of B6 and HO films, CS films had YS/G' values nearly 5-fold lower. Stress sweeps of CS and HO asphaltene systems after aging for 48 h are shown in Figure 10. While CS films had higher elasticities than HO films at comparable solvencies and aging times, their yield stresses were nearly 3-fold lower. The lower yield

(69) Ostlund, J. A.; Andersson, S. I.; Nyden, M. Studies of asphaltenes by the use of pulsed-field gradient spin echo NMR. *Fuel* **2001**, *80* (11), 1529–1533.



Figure 9. Top: View of the wrinkled film edge between the water and oil phases. The edge has extended into the oil phase and developed defects. Bottom: Film after oil removal. The large fragments resting on top of the film originated from the film edge, then extended upward into the oil phase, then fractured, and then fell off. The small triangular film pieces floating on top of the water phase were sheared off of the bulk film by the serrated bob edge.

stresses of CS films translated to YS/G' values close to 10, while HO films had values greater than 50. Loose connections between adjacent CS asphaltenic aggregates conferred interfacial elasticity, but under stress, the weak fabric holding the film together broke down more easily. As a result, CS films were quite brittle compared to HO and B6 films. The poor film formation of AH and CS asphaltenes suggests lower polarity than that of B6 and HO asphaltenes if one assumes that one of the key intermolecular forces which confers elasticity on asphaltenic films is hydrogen bonds. B6 asphaltenes, however, were less effective film formers in the *insoluble* regime, and the YS/G' ratio was much closer (18.3) to that of CS asphaltenes (10.1–12.1), suggesting that it is the most polar and hydrogen bonding fraction which precipitates from solution first as heptane concentration is increased. This is consistent with our recent findings.⁶⁴ The same convective forces applied successfully to pipet the oil phase from B6 and HO films apparently loosened and dispersed the CS film structure. Subsequently, no CS films were recovered. AH asphaltenic aggregates were too soluble to create elastic films or measurable film masses.

Asphaltene Fraction Rheology. Film properties of B6, HO, and CS precipitated asphaltenes are presented in Table 3. Limited solubility of these asphaltenes at

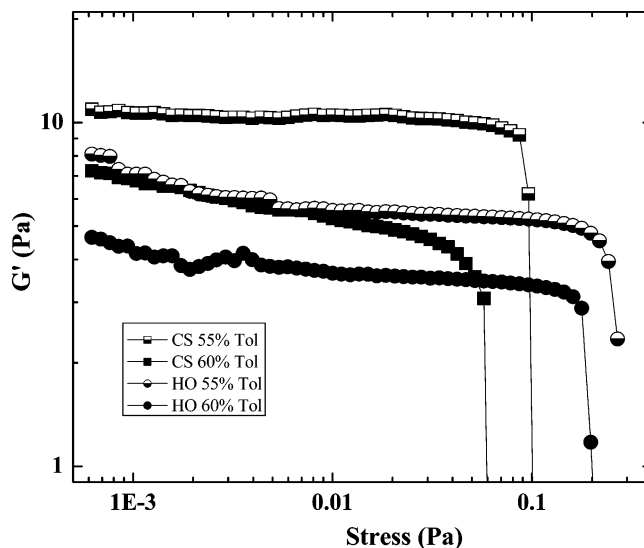


Figure 10. Stress sweeps of CS and HO whole asphaltenic film sweeps at 0.75% w/v, 1 rad/s, and after 48 h of adsorption and aging.

Table 3. Precipitate Asphaltene Film Properties in the Soluble Regime^a

asphaltene	% toluene	aging time (h)	G' (Pa)	yield stress (Pa)	film mass (g)	G'/mass (Pa/g)	YS/G' ($\times 10^{-3}$)
B6	100	48	28.37	0.834	0.0492	577	29.4
HO	80	48	17.36	0.750	0.0148	1170	43.3
	90	24	6.62	0.405	0.0066	1000	61.0
CS	90	144	2.525	0.0252			10.0

^a At 0.75% w/v in Heptol, 1 rad/s frequency.

intermediate toluene fractions precluded testing at these conditions. The elasticities of B6 and HO precipitate films at such high toluene volume fractions (0.8–1.0) were remarkable. This asphaltene fraction, though only slightly more aromatic and polar than the whole asphaltenes, was significantly more surface-active. Clearly, fractionation by Heptol solubility has isolated a group of asphaltenes capable of forming very elastic films and strong emulsions in highly aromatic solvents. HO precipitate formed films of particularly high consolidation, where the G'/mass ratio exceeded 1000 Pa/g and the YS/G' ratio was indicative of cohesion. B6 precipitate adsorbed more strongly, as suggested by the high film mass and the lower G'/mass value, than HO precipitate. CS precipitate was nearly incapable of elastic film formation even after 100 h of aging. Very large aggregates and poor solubility led to very weak consolidation and no cohesive, recoverable film.

Quantifying Film Consolidation and Adsorption. Several processes related to interfacial film formation were imbedded within the G' versus time trend, namely, adsorption, desorption, and consolidation. To determine how these processes impact film elasticity, we devised a solution replacement experiment in which asphaltenes adsorbed from solutions at an oil–water interface for discrete time periods and were then carefully removed by pipet. The interface was then rinsed delicately by trickling toluene down the glass cup onto the surface to remove any remaining asphaltenes in solution and to prevent further adsorption. Heptol solutions free of asphaltenes and at the same toluene volume fraction were then transferred to the interface. This procedure was performed at several time intervals on identical B6 whole asphaltene solutions in 60% (v/v) toluene in Heptol systems as well as on B6 precipitate asphaltene solutions in 100% toluene. The results of oil replacement are shown in Figures 11

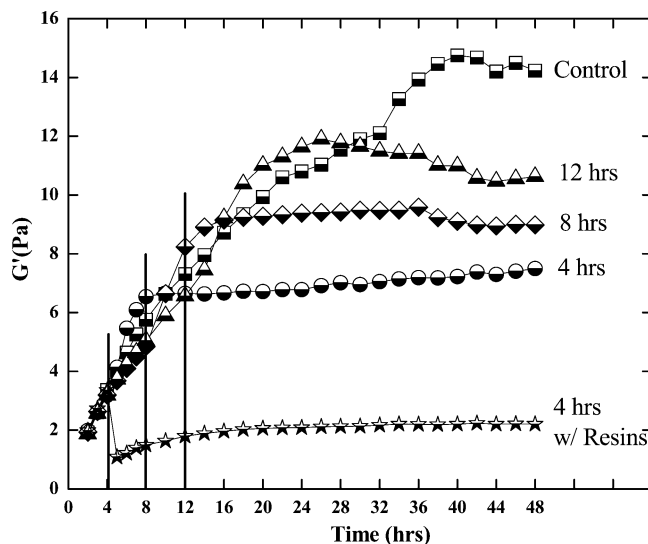


Figure 11. Kinetics of film elasticity changes during replacement of oil experiments with B6 whole asphaltenic films: 0.75% w/v, 60% toluene, 0.01 Pa, 1 rad/s. The graph labels refer to the contact time between the asphaltene solution and the water before replacing the oil phase with neat Heptol (or Heptol with resins).

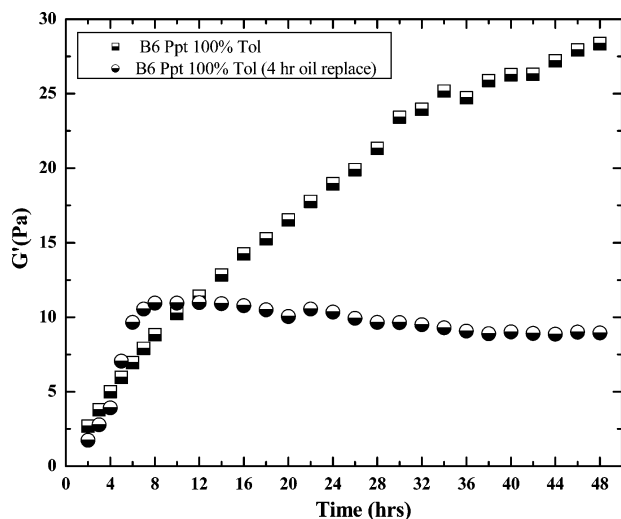


Figure 12. Kinetics of film elasticity changes during replacement of oil experiments with B6 ppt asphaltenic films: 0.75% w/v, 100% toluene, 0.01 Pa, 1 rad/s.

and 12. The control system showed some variations in film elasticity at the longest times as a result of the aforementioned tendency of well-formed films in the presence of an asphaltene solution to wrinkle at the cup wall.

The first oil replacement occurred after 4 h of interface aging in which the first three points represent film elasticities at 2, 3, and 4 h in the presence of asphaltenes. Following the frequency sweep at 4 h, the oil phase was replaced and the film left undisturbed for ~35 min until the 5 h frequency sweep. G' at 5 h was only slightly higher (0.1 Pa) than that in the control experiment. The increase in elasticity from 5 to 6 h was substantial and nearly 1 Pa higher than that in the control experiment. Film elasticity continued to rise in the absence of adsorbing asphaltenes until 12 h and varied little for the next 36 h. Between 4 and 12 h, G' was higher than the control possibly due to the applied convective forces during oil transfer. Molecular ordering and the process of interfacial consolidation continued for 12 h. Beyond 12 h, the asphaltenes

Table 4. Film Properties of B6 Whole and Precipitate Asphaltenes after Replacing the Oil Phase with Neat Heptol^{a,b}

fraction	replacement time (h)	G' (Pa)	yield stress (Pa)	film mass (g)	G'/mass (Pa/g)	YS/G' ($\times 10^{-3}$)
whole	none (72 h test)	17.22	0.770	0.0409	421	44.6
	12	6.78	0.405	0.0120	565	59.5
	8	5.73	0.405	0.0093	616	70.4
	4	4.78	0.365	0.0100	478	76.3
	4 w/ resins	2.20	0.106	0.0152	145	48.3
ppt	none (48 h test)	28.37	0.834	0.0492	577	29.4
	4	8.95	0.448	0.0187	479	50.0

^a At 0.75% w/v in Heptol, 1 rad/s frequency. ^b The first rows of the B6 whole and B6 precipitate data in the table refer to films aged in contact with asphaltene solution for 72 h and 48 h, respectively, and with no oil phase replacement. All replacement experiments aged for a total of 48 h.

in the film were likely in their final state of molecular ordering. Similar experiments after the 8 and 12 h frequency sweeps showed very similar results to those of the 4 h replacement experiment. These results clearly indicate that the consolidation process is crucial to conferring the ultimate elasticity that is measured for an asphaltenic film after adsorption occurs and some specific interfacial concentration of asphaltenes is obtained.

A fourth replacement experiment was performed in an attempt to desorb asphaltenes from the interface with a known asphaltenic solvent. A 0.75% w/v resin solution was prepared in 35 mL of a 40:60 (v/v) solution of Heptol. This solution was added to the film after pipetting the oil. The solvating and dissociating power of resins is evident, as G' fell significantly between the fourth and fifth hours. However, further desorption was not observed and the film began to consolidate under the new solvency conditions.

The final replacement experiment probed the degree of consolidation of the precipitate asphaltene fraction (Figure 12). After 4 h of aging, the B6 precipitate solution was removed from the cell and replaced with pure toluene. At the eighth hour, consolidation had ceased and G' was more than twice the magnitude of that at 4 h prior. Further testing revealed a very slight decrease in film elasticity over the next 40 h.

The G'/mass and YS/G' values for each of the films generated at long times in the oil replacement experiments of Figures 11 and 12 are listed in Table 4. The films subjected to rinsing had lower masses than the control film and correspondingly higher G'/mass values. This suggests that some of the additional asphaltenes adsorbed after 72 h of asphaltene solution contact did not necessarily contribute to film elasticity and resulted in lower overall consolidation. The G'/mass ratio of the resin experiment was noticeably lower than those of the resin-free films. It is likely that the resin solution was ineffective at removing asphaltenes from the interface but was able to disrupt the degree of film cohesion, perhaps by selectively solvating hydrogen bonding sites in the asphaltenes. Comparable YS/G' values suggested that the films were ostensibly similar in form and degree of consolidation.

Conclusions

Asphaltenic films formed at oil–water interfaces were successfully probed by interfacial shear rheometry with a serrated edge biconical bob. The films exhibited linear viscoelasticity and yield stresses. Elasticity and yield stress of the films increased with aging time and did not appear to reach equilibrium after several days due to a plentiful supply of asphaltenes. Many factors influenced

the degree of interfacial adsorption, elasticity, and yield stress. B6 and HO asphaltenes were the least aromatic, were the most polar (by nitrogen content), and had the highest concentrations of heavy metals (Ni and V). They formed films with a distinctive light-brown color, high elasticity, and high yield stress. Near the solubility limit, asphaltenes were highly aggregated and films formed rapidly and had considerable mass. In more aromatic solvents, interfacial adsorption was likely dominated by polar asphaltenes due to the high degree of solvent dispersion forces. These films did not form as quickly, and elasticity and yield stress at comparable aging times was lower. In the insoluble regime, precipitation hindered the adsorption process and measurable elasticities were obtained after much longer aging times. G' /film mass and yield stress/ G' values were used as measures of the degree of asphaltene consolidation. Films at high solvent aromaticity had higher G' /mass values, since the film masses were considerably lower than those of solvents near the asphaltene solubility limit. B6 and HO films also had high values of yield stress/ G' , indicating substantial consolidation and film strength.

AH and CS asphaltenes were more aromatic, were less polar, and had low concentrations of heavy metals. AH films were often too weak to measure. CS films were measurable but weaker than B6 or HO films. They did not possess the light-brown color and high degree of consolidation indicative of B6 or HO films either. CS films had such low consolidation that the adsorbed asphaltenes dispersed under convective forces during oil phase removal. In these cases, G' /film mass comparisons were not possible. Yield stress/ G' values indicated CS and AH films were more than 4 times weaker than B6 or HO films.

Film elasticities and yield stresses were also measured on fractionated asphaltenes. Fractionation concentrated the less soluble, more polar, and more aromatic asphaltenes with a greater propensity to adsorb at the oil-water interface. B6 and HO fractions formed film faster than unfractionated asphaltenes with higher elasticities at

comparable aging times in highly aromatic solvents. Adsorption at high solvent aromaticity was likely dominated by asphaltenes with considerable polarity and ability to form hydrogen bonds. Film consolidation exceeded that of the unfractionated asphaltenes as well.

Oil replacement experiments demonstrated the dual film formation processes of asphaltene adsorption and aggregate consolidation. After the asphaltene solution was removed and further adsorption was eliminated, film elasticity increased for several hours and then reached equilibrium. Films aged longer after solution replacement and had higher ratios of yield stress to G' , indicating enhanced consolidation. Replacing the oil phase with resins in Heptol rapidly reduced film elasticity due to film solvation.

The long time film elasticities and yield stresses of the asphaltenes correlate with the stability of emulsions formed at similar asphaltene concentrations and Heptol ratios. Asphaltenes are well solvated in highly aromatic solvents, form films of lower elasticity and yield stress, and form weaker emulsions. Enhanced aggregation near the solubility limit contributes to strong film and emulsion formation. B6 and HO asphaltenes have higher polarity and form well-consolidated films and strong emulsions. AH and CS have lower polarity and are poor film and emulsion formers. B6 and HO fractions of enhanced polarity form very strong films and emulsions even in highly aromatic solvents. These results strongly suggest that asphaltene chemistry dictates the properties of adsorbed films and that film shear elasticity and yield stress determine the strength of asphaltene stabilized water-in-oil emulsions.

Acknowledgment. This research was supported by funding from PERF (97-07), the National Science Foundation (CTS-981727), ExxonMobil, Ondeo-Nalco Energy Systems, Shell, and Texaco.

LA0356351